INTL JOURNAL OF ELECTRONICS AND TELECOMMUNICATIONS, 2026, VOL. 72, NO. 2, PP. 1-6
Manuscript received May 5, 2026; revised May 2026. doi: 10.24425/ijet.2026.157940

I–V Characteristics of ISFET Devices in Iron(II) Fumarate Solutions

Piotr Firek, and Piotr Niedzielski

***Abstract*— This work presents the fabrication process and I–V characteristics of ISFET devices with an open gate. Measurements were performed in deionized water and in deionized water solutions containing iron(II) fumarate at various concentrations. Changes in the electrical parameters of the transistors were analyzed as a function of electrolyte composition, with particular emphasis on the influence of Fe^{2+} ions and fumarate anions. The study aimed to assess the sensitivity and stability of ISFET devices in a complex ionic environment.**

***Keywords*— ISFET; I–V characteristics; iron(II) fumarate; ion-sensitive transistor; electrolyte interface; multicomponent ionic environment**

I. Introduction

THE study of ISFET response in complex ionic environments is essential for understanding how multiple ions and electrostatic interactions influence sensor performance.

Ion-sensitive field-effect transistors (ISFETs) are widely used as chemical sensors due to their ability to detect changes in ion activity at the electrolyte-insulator interface. Their response is governed by surface potential variations, which depend on the composition of the surrounding electrolyte.

Early ISFET development focused on adapting the MOSFET concept for ion detection, primarily using silicon dioxide (SiO_2) as the gate insulator [1]. However, alternative high-k materials have been explored to improve sensitivity and stability. For example, aluminum oxide (Al_2O_3) layers on nanoISFET devices have demonstrated near-Nernstian pH response, significantly exceeding the performance of conventional SiO_2 layers [2]. Modeling studies further indicate that materials such as Al_2O_3, tantalum pentoxide (Ta_2O_5), and zirconium dioxide (ZrO_2) exhibit enhanced surface potential response compared to SiO_2, making them attractive candidates for improved ISFET performance [3]. Recent reviews note that a variety of metal oxide materials (e.g., Si_3N_4, AlN, Al_2O_3, Ta_2O_5, HfO_xN_y, $BaTiO_3$) have been investigated as sensitive membranes due to their impact on device characteristics [4][5][6][7]. Beyond typical dielectric layers, our previous work investigated sensing potential across a broad thickness spectrum - ranging from several hundred nanometers to the true atomic limit - focusing on carbon-palladium (C-Pd) nanocomposites and graphene-based structures [8][9].

While the behaviour of ISFETs in simple electrolyte solutions such as KCl, NaCl, or HCl is well documented, their response in more complex ionic environments remains less understood. Several studies have shown that the presence of multiple ions, organic anions, or counter-ions can significantly influence the device characteristics due to changes in the surface potential and the formation of complex electrostatic interactions at the electrolyte-insulator interface (e.g., [10], [11], [12]). However, few works have explored systems combining metal cations with organic dianions, which are relevant for understanding sensor performance in multicomponent ionic media. The present study investigates aqueous solutions of iron(II) fumarate as a model system to examine ISFET response under such conditions.

Among complex ionic systems, iron(II) fumarate solutions are particularly interesting because they combine metal cations with an organic dianion. The Fe^{2+} ion may participate in oxidation processes, while the fumarate ion influences the ionic balance, charge distribution, and buffering properties of the solution. In addition, interactions between Fe^{2+} ions and fumarate anions may lead to the formation of transient complexes near the sensing surface.

Such behaviour may significantly affect the surface potential at the electrolyte–insulator interface and, consequently, the electrical response of the ISFET device. In contrast to simple electrolytes, the Fe^{2+}-fumarate system creates a more complex ionic environment in which both electrostatic and redox-related effects may contribute to the measured signal.

Although many studies have examined ISFET operation in simple salt solutions or pH-buffered media, relatively few works have focused on systems containing both metal ions and organic anions. Therefore, such solutions may provide a useful model for studying ISFET behaviour in multicomponent ionic environments.

The aim of this work was to investigate the I-V characteristics of ISFET devices in aqueous solutions containing different concentrations of iron(II) fumarate and to evaluate the influence of this complex ionic system on the electrical response of the structures.

II. Experimental Details

A. ISFET structures preparation

Open-gate field-effect transistors were fabricated using a standard silicon transistor process with an aluminum gate. However, in the final metallization step, the gate area was intentionally left exposed.

Piotr Firek is with Warsaw University of Technology, Institute of Microelectronics and Optoelectronics Warsaw, Poland (e-mail: piotr.firek@pw.edu.pl).

Piotr Niedzielski is with Łodz University of Technology, Institute of Materials Science and Engineering, Poland

1) Substrate preparation and field oxide growth

In the first stage of the process, p-type silicon wafers with <100> orientation and a resistivity of 1-10 Ωcm were cleaned and stripped of the native oxide layer. The wafers were then subjected to thermal oxidation in a steam atmosphere (HYDROX process). The resulting field oxide thickness was approximately 700 nm - Fig. 1a.

2) Photolithography I - definition of source and drain regions

A positive photoresist was deposited onto the wafers and spin-coated to obtain a uniform layer approximately 1 µm thick. The photoresist was subsequently soft-baked at 80°C for 30 minutes. Proximity photolithography was applied, with an exposure time of 8 seconds.

After exposure, the wafers were immersed in the developer solution for 1 minute, rinsed in deionized water, and spin-dried. The photoresist was then hard-baked at 120°C for 30 minutes in order to improve adhesion to the SiO_2 surface and remove residual solvent.

The field oxide not protected by the photoresist was etched in a buffered hydrofluoric acid solution consisting of HF and NH_4F mixed in a 1:6 ratio. Finally, the photoresist was removed in acetone, followed by rinsing in deionized water and spin drying, which completed the photolithography process.

3) Phosphorus diffusion in source and drain regions

All diffusion processes were carried out at a temperature of 960°C under atmospheric pressure conditions. The first step consisted of oxidation of the wafers, specifically the exposed source and drain areas, for 6 minutes with nitrogen and oxygen flow rates of 3.5 dm^3/min and 0.35 dm^3/min, respectively. Next, phosphorus predeposition was performed for 15 minutes using nitrogen and oxygen flow rates of 0.06 dm^3/min and 0.35 dm^3/min, respectively. Phosphorus was supplied by passing nitrogen through a $POCl_3$ solution, which acted as the dopant source. The drive-in diffusion process was then carried out for 5 minutes with nitrogen and oxygen flow rates of 3.5 dm^3/min and 0.35 dm^3/min, respectively.

After completion of the diffusion process, the phosphosilicate glass layer formed on the wafer surface was removed in a buffered HF:NH_4F solution (6:1) for 15 seconds (Fig. 1b).

4) Photolithography II - definition of active regions

At this stage, mask alignment with respect to the previously formed structures on the wafer surface was required.

The process of exposing the active regions was identical to the oxide removal procedure used for the source and drain regions. The wafers were immersed in buffered HF solution for 6 minutes and 30 seconds in order to remove the oxide from the defined active areas (Fig. 1c).

5) Substrate preparation prior to gate dielectric formation

The cleaning procedure consisted of five stages. After each stage, the wafers were rinsed in deionized water in order to remove residual chemicals.

A) Preliminary cleaning was performed in an H_2O_2:H_2SO_4 solution with a volume ratio of 1:2 for 5 minutes.

B) Organic contaminants were removed using the SC-1 solution for 10 minutes. The solution consisted of H_2O:NH_4OH:H_2O_2 mixed in a 5:1:1 ratio. The process was carried out at a temperature of approximately 80°C.

C) Remaining contaminants, mainly metallic impurities, were removed using the SC-2 solution for 10 minutes. The solution consisted of H_2O:HCl:H_2O_2 mixed in a 6:1:1 ratio. The process was also performed at approximately 80°C

D) A thin oxide layer formed during the previous cleaning processes was removed using an HF:H_2O solution with a ratio of 1:50 for approximately 15 seconds.

E) Finally, the wafers were spin-dried.

6) Gate dielectric formation

A silicon dioxide gate dielectric layer with a thickness of approximately 20 nm was formed by thermal oxidation. The oxidation process was carried out in thermal oxidation at atmospheric pressure at a temperature of 1000°C with an oxygen flow rate of 0.2 dm^3/min for 10 minutes (Fig. 1d).

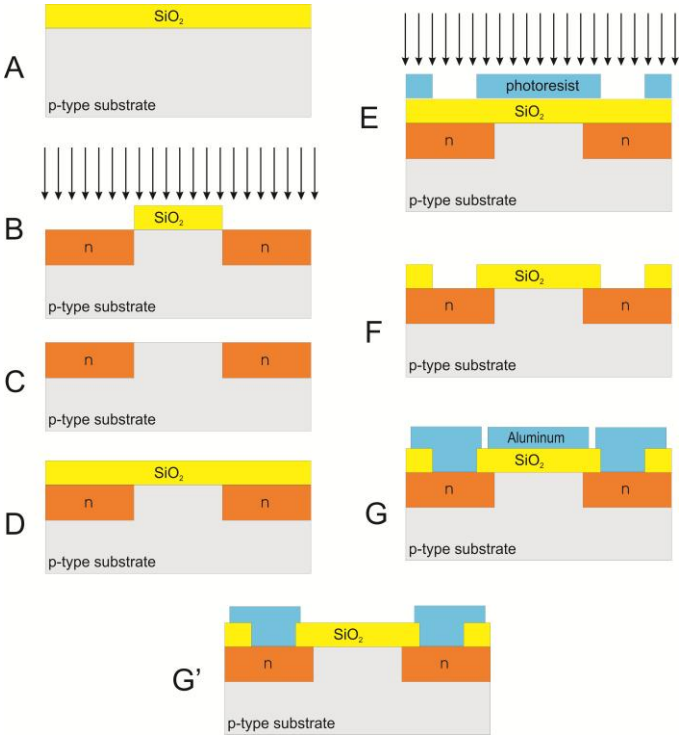

Fig. 1. Preparation of the MIS/ISFET structures.

7) Photolithography III - contact formation

In case the third photolithography process, the openings in the chromium layer of the photomask corresponded to the contact regions.

8) Removal of the dielectric layer from the source and drain regions

The silicon dioxide layer was removed from the source and drain contact areas by wet etching in buffered HF solution for 2 minutes (Fig. 1e-f).

9) Aluminum deposition

An aluminum layer was deposited onto the wafer surface by vacuum evaporation. The deposition process was carried out in at a pressure of approximately 3×10^{-6} Torr and lasted 2 minutes. The vacuum was generated using a two-stage pumping system consisting of a rotary pump and a diffusion pump.

10) Photolithography IV – aluminum metallization patterning

The patterns defined in the photomask corresponded to the final metallization topology. In this step, the aluminum layer was etched using a solution composed of H_3PO_4:CH_3COOH:H_2O:HNO_3 mixed in a 31:6:2:1 ratio. The etching process lasted approximately 3 minutes (Fig. 1G and G').

The fabrication process of ion-sensitive ISFET transistor structures was identical to that used for MISFET devices. The presented technology enabled the fabrication of two types of transistor structures on the same silicon wafer by applying different metallization masks during the final photolithography stage.

As a result, structures with a conventional aluminum gate as well as open-gate devices without gate metallization were obtained. Fig. 2 presents the topology of the ISFET structures after subsequent fabrication stages. The fabricated ISFET and MISFET structures on a silicon wafer are presented in Fig. 3.

Fig. 2. Topography of the ISFET structures obtained after subsequent stages of the fabrication process.

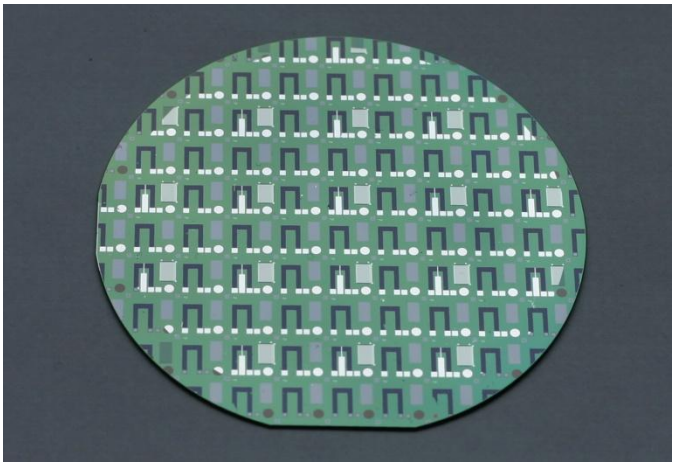

Fig. 3. Silicon wafer with fabricated ISFET and MISFET structures.

B. Packaging

The transistor structures were mounted onto dedicated PCB substrates using a single-component polyimide adhesive with silver filler, EPO-TEK P-1011. Electrical interconnections were then formed by ultrasonic wire bonding using aluminum wire with a diameter of 100 μm.

The bonding process combines ultrasonic energy with mechanical pressure. The pressure is applied by a sonotrode, which transfers vibration energy from the generator through a transducer and a vibration transformer. Ultrasonic vibrations in the contact region produce friction between the joined surfaces, resulting in local heating, wire deformation, and enhanced atomic diffusion, which together lead to the formation of a mechanically stable and electrically reliable bond.

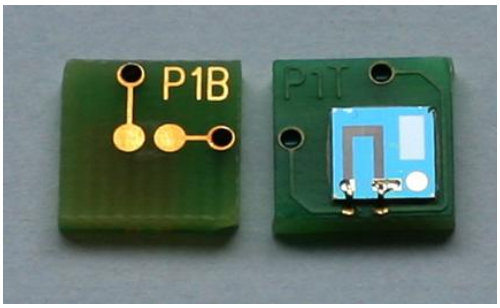

Fig. 4. Mounted ISFET structure with completed wire bonds.

After the bonding process, the wire connections were protected with semiconductor-grade silicone in order to reduce the mechanical sensitivity of the system.

Fig. 4 shows a mounted ISFET structure with completed wire bonds and protective coating, ready for electrical measurements.

C. Measurements

A standard measurement setup dedicated to the analysis of ISFET structures with ion-sensitive membranes fabricated from various materials was used in this study. The system performed three main functions: it provided controlled liquid flow in the measurement cell, enabled electrical characterization of the devices, and allowed data visualization and storage.

A reference electrode immersed in the solution was used to control the gate potential in the range from -5 V to +5 V with a step of 0.25 V. The drain–source voltage and drain current were measured or applied using a Keithley 236 Source Measure Unit (SMU). Measurement conditions, data acquisition, visualization, and analysis were carried out using Metrics ICV software.

The measurements were carried out in two stages. In the first stage, the operation of the structures was evaluated by measuring transfer and output characteristics in deionized water. This preliminary step made it possible to select only properly functioning devices with stable electrical parameters for further investigation. In the second stage, the output characteristics were measured in iron(II) fumarate.

Four iron(II) fumarate solutions in deionized water were prepared. The first solution contained 25 mg of iron(II) fumarate, the second 50 mg, the third 75 mg, and the fourth 100 mg. Current-voltage characteristics were measured for all transistors at each concentration.

The possibility of detecting iron(II) fumarate in solution was investigated by comparing the I-V characteristics obtained in deionized water with those measured in iron(II) fumarate solutions. The measurements were performed consecutively in order to minimize the influence of changes in device condition over time. The I-V curves for deionized water and iron(II) fumarate solutions were plotted together to provide a clearer visualization of the observed differences. The analyzed parameter was the channel current flowing between the drain and source

III. Results

Fig. 5a presents the typical I-V characteristics of ISFET structures measured in deionized water. The characteristics obtained for the 0.025% iron(II) fumarate solution are shown in Fig. 5b.

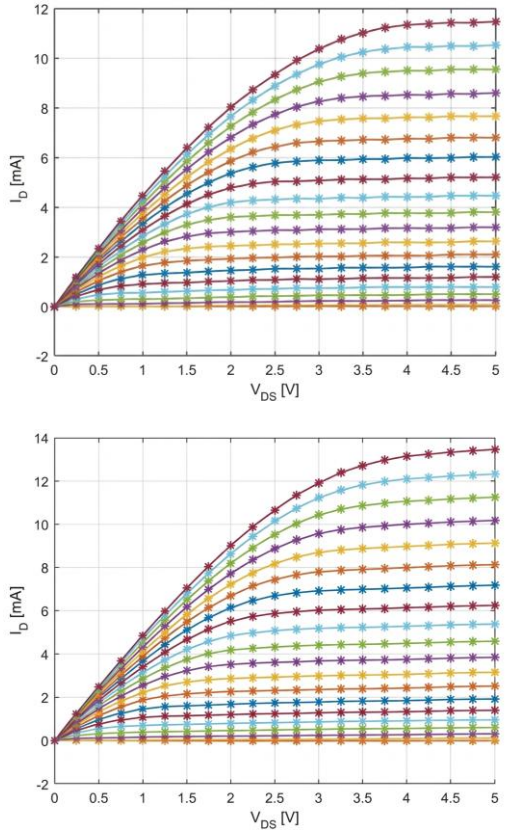

Fig. 5. Typical I-V characteristics of ISFET structures measured in a). deionized water b) iron(II) fumarate solution.

Analysis of the obtained characteristics indicates that the detection of iron(II) fumarate in deionized water is possible. The vast majority of the measured transistors (approximately 90%) exhibited a higher drain current in iron(II) fumarate solutions than in deionized water. The variations in drain current were most pronounced for drain-source voltages (VDS) in the range of 4-5 V. Similarly, the most favourable gate polarization conditions for observing the sensor response were obtained within the same voltage range.

The feasibility of characterizing and quantifying iron(II) fumarate concentration in solution was evaluated by analysing differences in the drain current (I_D) between measurements performed in deionized water and in analyte solutions. The investigated concentration range included 0.025%, 0.05%, 0.075%, and 0.1% iron(II) fumarate solutions. For each device, current-voltage characteristics were recorded for all four iron(II) fumarate concentrations. Changes in the drain current in response to varying concentrations of the iron fumarate solution were also recorded. (Fig. 6).

The obtained results demonstrate that the presence of iron(II) fumarate consistently leads to an increase in drain current. However, no clear monotonic relationship between analyte concentration and electrical response was observed. In some cases, larger current changes occurred for lower concentrations, while higher concentrations produced smaller variations.

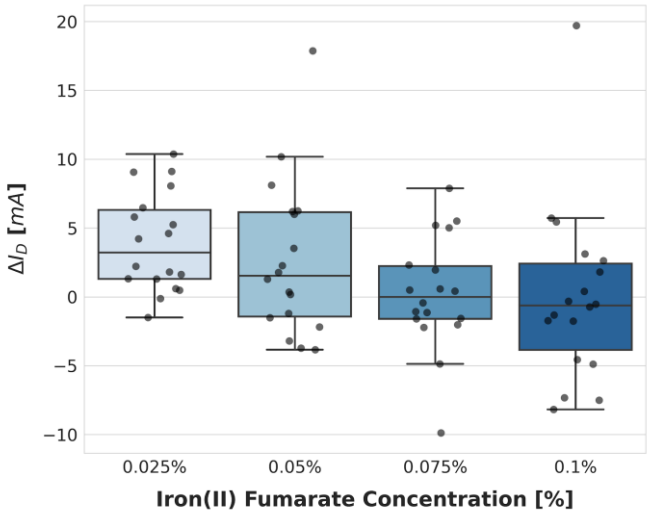

Fig. 6. Drain current changes as a function of iron(II) fumarate solution concentration.

An examination of individual device profiles reveals a predominant 'peak-and-decline' behavior (Fig. 7), where the maximum response is often achieved at lower concentrations (0.025%-0.05%). This non-monotonicity confirms that the sensing mechanism is dominated by surface adsorption kinetics rather than bulk concentration. A further increase in iron(II) fumarate concentration likely leads to the saturation of available binding sites on the gate dielectric or potential charge screening effects, resulting in a diminished electrical response (Fig. 7).

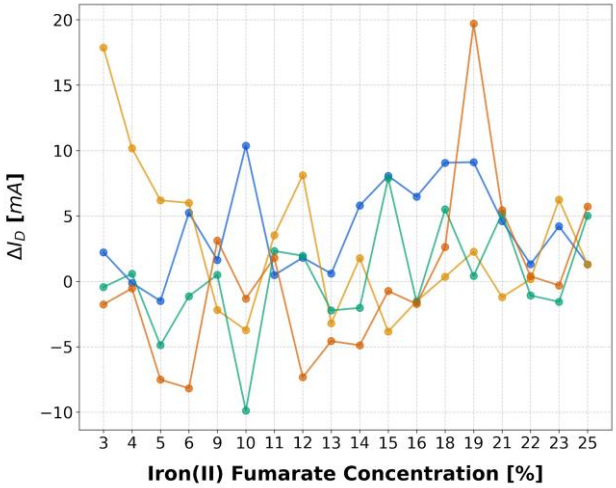

Fig. 7. Individual response of ISFET structures across the investigated iron(II) fumarate concentration range (0.025%-0.1%).

The obtained results indicate that, although the presence of iron(II) fumarate consistently leads to an increase in the drain current, a clear monotonic relationship between the analyte concentration and the electrical response was not observed. In some cases, larger changes in drain current were recorded for lower concentrations, while higher concentrations resulted in smaller variations.

This behaviour suggests that the ISFET response is not determined solely by the bulk concentration of the analyte, but is strongly influenced by interfacial phenomena occurring at the electrolyte-insulator boundary. In particular, adsorption of Fe^{2+} ions or fumarate anions at the sensing surface, as well as possible formation of surface complexes, may lead to non-linear and device-dependent responses.

The results further indicate that the investigated structures are more suitable for qualitative detection of iron(II) fumarate presence than for precise quantitative concentration analysis under the current experimental conditions. The sensor response appears to behave more like a threshold-type detection mechanism, where the presence of the analyte produces a measurable electrical effect, while accurate concentration discrimination remains limited. This is further evidenced by the relative sensitivity analysis (Fig. 8), which shows significant signal enhancement even at the lowest tested concentrations, followed by a saturation-like decline.

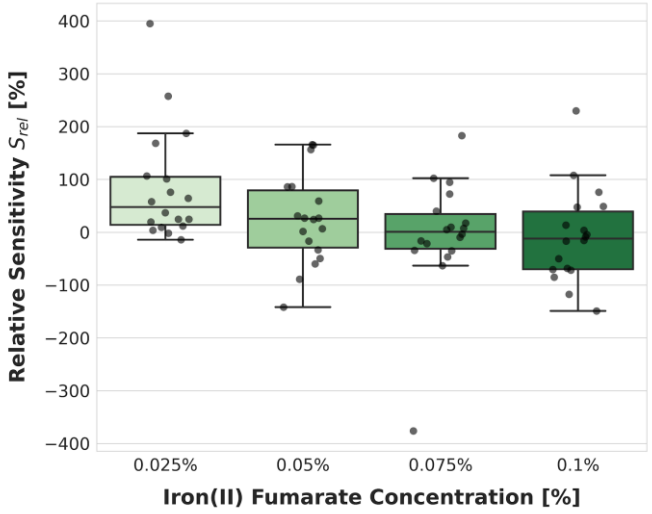

Fig. 8. Relative sensitivity S_{rel} of the measured ISFET structures, calculated as the percentage change in drain current relative to the deionized water baseline.

The variability observed between individual transistors suggests high sensitivity to local surface conditions, dielectric quality, and history-dependent effects. In some cases, differences between individual devices were comparable to or greater than the variations caused by changes in analyte concentration. Such behaviour is characteristic of surface-sensitive devices operating in complex ionic environments and indicates the dominant role of surface-related phenomena.

A likely contributing factor is insufficient regeneration of the sensing surface between successive measurements. Currently, the transistors are only rinsed with deionized water and dried, which may not effectively remove adsorbed species from the dielectric surface. This can lead to memory effects, hysteresis, and parameter drift during subsequent measurements.

To improve repeatability and enable more reliable quantitative analysis, the development of an effective surface regeneration protocol is required. Potential approaches include the use of low-pH rinsing solutions or chelating agents to promote desorption of iron ions from the dielectric surface. Recent studies emphasize the role of ethylenediaminetetraacetic acid (EDTA) as a particularly effective chelating agent due to the high stability and favorable thermodynamics of iron-EDTA complexes [13, 14]. The application of such agents can selectively sequester adsorbed metal ions, thereby restoring the surface potential of the gate dielectric. The method previously proposed in [15] does not prove effective in all cases and may require adaptation depending on the specific sensing conditions.

Despite the observed limitations, the obtained results confirm that ISFET structures can be used to investigate sensor response in multicomponent ionic systems extending beyond simple electrolyte solutions.

CONCLUSION

The presented results demonstrate that ISFET devices with an open gate configuration are sensitive to the presence of iron(II) fumarate in aqueous solutions. In the majority of the tested structures, an increase in drain current was observed in comparison to measurements performed in deionized water, indicating a measurable influence of the analyte on the surface potential at the electrolyte–insulator interface.

The observed changes can be attributed to the combined effect of Fe^{2+} ions and fumarate anions, which modify the charge distribution and electrostatic conditions near the sensing surface. The Fe^{2+}-fumarate system thus represents a simple model of a multicomponent ionic environment affecting ISFET response.

Although the results confirm the possibility of detecting iron(II) fumarate, a clear and monotonic relationship between concentration and electrical response was not obtained. This limitation is likely related to surface effects such as ion adsorption and insufficient regeneration of the sensing layer, leading to memory effects and reduced repeatability.

Future work should focus on the development of effective surface regeneration procedures and improved measurement protocols to enhance reproducibility and enable quantitative analysis.

ACKNOWLEDGEMENTS

The author would like to acknowledge the support provided by the Institute of Materials Science and Engineering at the Lodz University of Technology during a research internship. Thank you to Natalia Dołba for her support in carrying out the measurements.

REFERENCES

[1] P. Bergveld, "Thirty years of ISFETOLOGY, What happened in the past 30 years and what may happen in the next 30 years, " Sensors and Actuators B: Chemical, vol 88, (1), pp. 1–20, 2003, https://doi.org/10.1016/S0925-4005(02)00301-5

[2] Meng-Nian Niu, Xin-Fang Ding and Qin-Yi Tong, “Effect of two types of surface sites on the characteristics of Si_3N_4-gate pH-ISFETs,” Sensors and Actuators B: Chemical, vol. 37 (1–2), pp. 13-17, 1996, https://doi.org/10.1016/S0925-4005(97)80067-6.

[3] P. Zenita, A.B. Devi, K.J. Singh and N.B. Singh, “Modeling and performance analysis of high-k gate material-based isfet biosensors using

TCAD," Journal of Computational Electronics, vol 24, pp. 197-206, 2025, https://doi.org/10.1007/s10825-025-02434-y

[4] S. Yoshida, N. Hara, and K. Sugimoto, "Development of a Wide Range pH Sensor based on Electrolyte-Insulator-Semiconductor Structure with Corrosion-Resistant Al_2O_3, Ta_2O_5 and $Al_2O_3ZrO_2$ Double-Oxide Thin Films," Journal of The Electrochemical Society, vol. 151, pp. H53-H58, 2004, https://doi.org/10.1149/1.1643074

[5] P. Firek, G. Głuszko, L. Łukasiak, J. Szmidt, A. Jakubowski, and M. Sochacki, "Charge pumping characterization of MISFETs with SiO_2/$BaTiO_3$ as a gate stack," Przegląd Elektrotechniczny, vol. 90, no. 9, pp. 26–28, 2014, https://doi.org/10.12915/PE.2014.09.08

[6] P. Firek, M. Waśkiewicz, B. Stonio and J. Szmidt, "Properties of AlN thin films deposited by means of magnetron sputtering for ISFET applications," Materials Science-Poland, vol. 33, pp 669-676, 2015, https://doi.org/10.1515/msp-2015-0095

[7] P. Firek, P. Wysokiński, "Manufacturing of HfO_xN_y films using reactive magnetron sputtering for ISFET application," Proceedings SPIE, vol. 10175, 1017507, 2016, https://doi.org/10.1117/12.2261660

[8] 12. P. Firek, S. Krawczyk, H. Wronka, E. Czerwosz and J. Szmidt, "Hydrogen sensor based on field effect transistor with C-Pd layer," Metrology and Measurement Systems, vol. 27, no. 2, pp. 313–321, 2020, https://doi.org/10.24425/mms.2020.132777

[9] K. Kondracka, P. Firek, P. Caban, A. Przewłoka and J. Szmidt, "Technology and Characterization of ISFET Structures with Graphene Membrane," Proceedings of SPIE, vol. 11176, pp., 1–7, 2019, https://doi.org/10.1117/12.2536746

[10] K. Parizi, X. Xu, A. Pal, X. Hu and H. S. P. Wong, "ISFET pH Sensitivity: Counter-Ions Play a Key Role,", Scientific Reports vol. 7, 41305, 2017, https://doi.org/10.1038/srep41305

[11] I Poels, R.B.M Schasfoort, S Picioreanu, J Frank, G.W.K van Dedem, A van den Berg and L.J Nagels, "An ISFET-based anion sensor for the potentiometric detection of organic acids in liquid chromatography," Sensors and Actuators B: Chemical, vol. 67 (3), pp. 294-299, 2000, https://doi.org/10.1016/S0925-4005(00)00531-1

[12] J. Zou, H. Bai, L. Zhang, Y. Shen, C. Yang, W. Zhuang, J. Hu, Y. Yao and W. Hu "Ion-sensitive field effect transistor biosensors for biomarker detection: current progress and challenges," Journal of Materials Chemistry B, vol. 12, pp. 8523-8542, 2024, https://doi.org/10.1039/D4TB00719K

[13] S. Falina, M. Syamsul, N. A. Rhaffor, S. Sal Hamid, K. A. Mohamed Zain, A. Abd Manaf, and H. Kawarada "Ten Years Progress of Electrical Detection of Heavy Metal Ions (HMIs) Using Various Field-Effect Transistor (FET) Nanosensors: A Review," Biosensors, vol. 11, no. 12, p. 478, 2021, https://doi.org/10.3390/bios11120478

[14] K. Zhang, Z. Dai, W. Zhang, Q. Gao, Y. Dai, F. Xia, X. Zhang, "EDTA-based adsorbents for the removal of metal ions in wastewater," Coordination Chemistry Reviews, vol. 434, p. 213809, 2021, https://doi.org/10.1016/j.ccr.2021.213809

[15] K. Kondracka, P. Firek, M. Grodzik, M. Szmidt, E. Sawosz–Chwalibóg and J. Szmidt, "Influence of Multiple Cleaning on the Detection Capabilities of ISFET Structures," International Journal of Electronics and Telecommunications (IJET), vol. 67, 1/2021, https://doi.org/10.24425/ijet.2021.135939